Final Technical Progress Report

SUBMITTED TO

U.S. Department of Energy
Office of Fossil Energy
National Energy Technology Laboratory
Project Manager Sai Gollakota

July 31, 2018

Maximizing Current Density for Electrochemical Conversion of Flue Gas CO_2 to Ethanol

Field Work Proposal # FEAA132

SUBMITTED BY

Oak Ridge National Laboratory
P.O. Box 2008
Oak Ridge, TN 37831-6156
DUNS# 099114287

Grant Period 8/15/2017 to 7/31/2018

PRINCIPAL INVESTIGATOR

Dr. Adam J. Rondinone
(865) 574-5035
(865) 335-9032
rondinoneaj@ornl.gov

Signature

Adam J. Rondinone

Acknowledgment: This material is based upon work supported by the Department of Energy under Field Work Proposal: #FEAA132.

Acronyms

C2	Any molecule containing 2 carbon atoms
CNS	Carbon nanospikes
CO_2RR	CO_2 reduction reaction
FE	Faradaic efficiency
GDE	Gas diffusion electrode
MEA	Membrane-electrode assembly
NMR	Nuclear magnetic resonance
NO_x	Nitrogen-oxide species
OER	Oxygen evolution reaction
PEMFC	Proton-exchange membrane fuel cell
ppm	Part per million
SO_x	Sulfur-oxide species
XPS	X-ray photoelectron spectroscopy

Tasks and Budgets

				FY2017	FY2018			
	Start Date	End Date	Cost	4	1	2	3	4
Task 1. Project Management and Planning*	8/15/2017	7/31/2018						
Quarterly report				12/31/17	3/31/28	6/31/18		
Comprehensive Final Report							7/31/18	
Task 2.1 Maximize current density of catalyst for production of ethanol – 3D electrode development	8/15/2017	9/30/2017	$71,000					
Task 2.2. Maximize current density of catalyst for the production of ethanol – 3D electrode, gas phase operation, maximize wettability	10/1/2017	7/31/2018	$49,000					
Milestone: Configure catalyst for gas phase operation					1/31/28		7/31/18	
Milestone: Complete maximization of current density of catalyst								
Task 3. Measure and optimize performance in flue gas	11/1/2018	7/31/2018	$80,000					
Milestone: Test and optimize catalyst against flue gas impurities					3/31/2018			
Milestone: Complete characterization of impurity intolerances							7/31/18	

	Fiscal Year 1				**Fiscal Year 2**					
	8/15/17 – 9/30/17		10/1/17 – 12/31/17		1/1/18 – 3/31/18		4/1/18 – 6/30/18		7/1/18 – 7/31/18	
	Q1	Total Project	Q2	Total Project	Q3	Total Project	Q4	Total Project	Q5	Total Project
Federal Share	$71,000	$71,000	$33,000	$104,000	$43,000	$147,000	$43,000	$190,000	$10,000	$200,000
Total Planned	$71,000	$71,000	$33,000	$104,000	$43,000	$147,000	$43,000	$190,000	$10,000	$200,000

Introduction

Closing the carbon cycle by developing ways to recycle carbon dioxide (CO_2) into useful products may be a way to reduce or eliminate the environmental impact of fossil fuels. Direct electrochemical conversion of CO_2 to useful products has been under investigation for more than four decades, but a significant challenge has been a lack of electrochemical catalysts that could achieve high product selectivity. In our previous study (*1*), a prototype cell with 1 cm^2 carbon nanospike (CNS, see ref (*2*)) cathode with electronucleated Cu nanoparticles (Cu/CNS) was shown to have higher selectivity for CO_2 electroreduction (84%) than H_2 evolution, with a subsequent high Faradaic efficiency (FE) towards ethanol (60-65%). This achievement was significant because electrochemical synthesis of ethanol requires a 12-electron CO_2 reduction reaction (CO_2RR) with H_2O as a proton source:

$$2\,CO_2 + 9\,H_2O + 12\,e^- \rightarrow C_2H_5OH + 12\,OH^-$$

Where the anodic reaction is the oxygen evolution reaction (OER).

$$2\,H_2O \rightarrow O_2 + 4\,H^+ + 4\,e^-$$

The overall current was relatively low (~ 2 mA/cm^2) and expensive monocrystalline Si wafer substrate was used for CNS deposition. Together these facts limited this technology for industrial applications. For the purposes of the Fossil Energy program, we set out to study ways to raise the current density of the catalyst and understand the catalyst operation in the context of typical contaminants that would be present in coal combustion flue gas.

Results

Initially we studied the growth and operation of the catalyst on a variety of metallic substrates that could support non-planar geometries. This approach was a critical part of raising the current density, by texturizing and deepening the interface between the catalyst surface and the electrolyte. According to our experience, CNS can be deposited onto any conductive substrate. The metallic substrates tested here included stainless steel, titanium and copper sheet. Unfortunately, our investigation revealed that metal atoms in stainless steel, such as iron, nickel and chrome can migrate into CNS during the chemical vapor deposition process used to synthesize the CNS. These metals have an affinity towards the hydrogen evolution reaction and lead to higher hydrogen selectivity. With additional investment, a buffer layer could probably be devised, but for this short-term project we decided to move on to alternatives. CNS deposition on high purity copper and titanium substrates revealed CNS with the desired morphology and composition and no metal contamination. While copper and titanium can support high purity CNS layers, they ultimately failed during long term experiments, because the interface between the metal substrate and the CNS layer was subject to electrochemical remodeling. Once the remodeling process started, the CNS layer was no longer adhered to the surface and the reaction mechanism would break down. Graphitic carbon, which is stable under reaction conditions, was selected as a more suitable substrate. Graphite also has the advantage of being highly conductive, physically stable, and in principle absent of any undesired metals. We have now successfully deposited CNS on isostatically pressed graphite plates, carbon cloth, carbon paper and carbon fibers. The carbon cloth, the carbon plate and the original CNS on monocrystalline silicon are shown in Figure 1. In an accelerated durability study (whole cell potential 5.1 V) the CNS were shown to be remarkably stable on a graphite plate with no evidence of delamination over the course of a 300-hour experiment. Figure 2 shows a cross section of the graphite electrode with the CNS coating after the durability study. We hypothesize that the chemical similarity between the graphite and the nitrogen-doped graphene sheets of CNS leads the superior adhesion. Metallic impurities (0.05% ash) and structural imperfections in commercial graphite may affect the chemical selectivity, which will necessitate using an ultra-high purity grade.

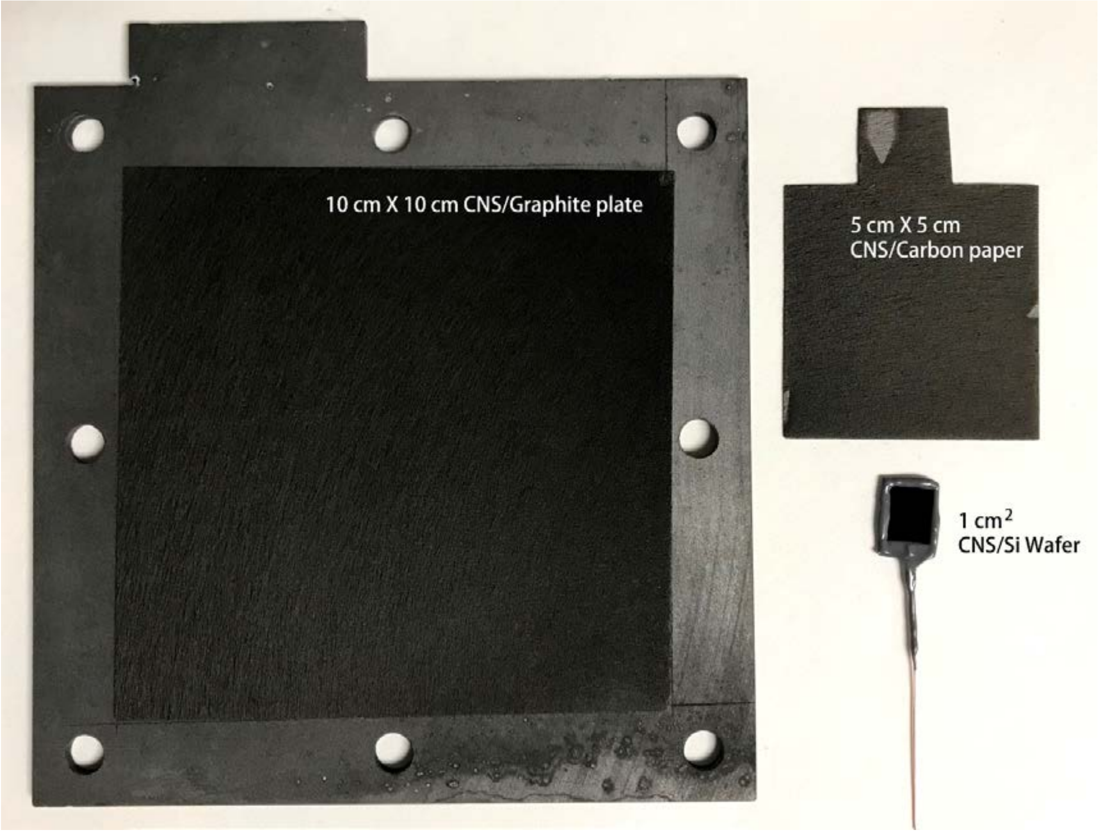

Figure 1. Examples of electrode types used in this study: (left) 100 cm^2 CNS on graphite plate, (top right) 25 cm^2 CNS on carbon paper, (bottom right) original 1 cm^2 CNS on Si wafer. Black paper on the large graphite electrode (left) is a visual aid to illustrate the active area of the electrode.

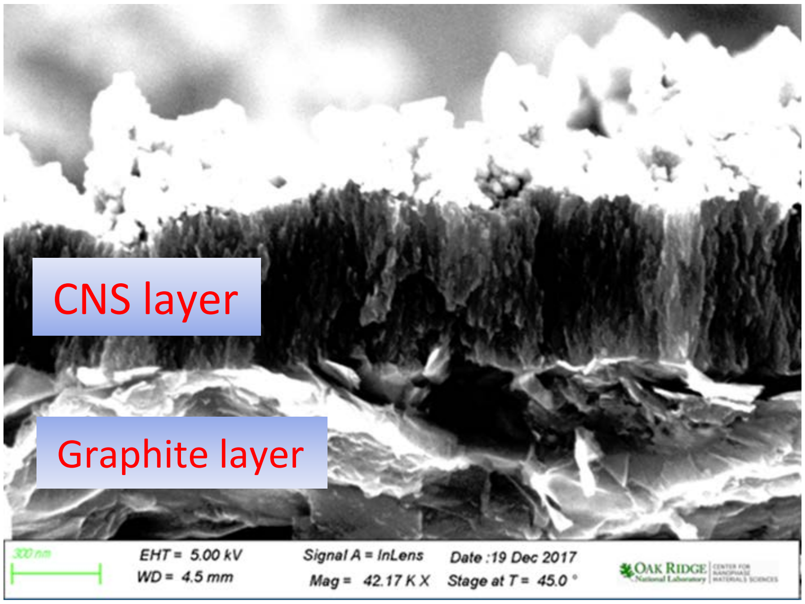

Figure 2. SEM image of the isostatically pressed graphite coated with the CNS after 300-hour accelerated durability study. In multiple runs no delamination was noted.

The difficulty encountered with metallic substrates and success using graphite suggested that the best path forward for higher current density would be to utilize a gas diffusion electrode (GDE) cell for the electrochemical CO_2 reduction in the vapor phase. Vapor phase cells have been demonstrated to greatly increase the current density of many electrochemical catalysts, if the catalyst can be adapted to run in the vapor phase. Like a proton-exchange membrane fuel cell (PEMFC), the vapor cell was composed with two graphite blocks acting as both current collector and gas dispenser, and a membrane electrode assembly (MEA). The MEA

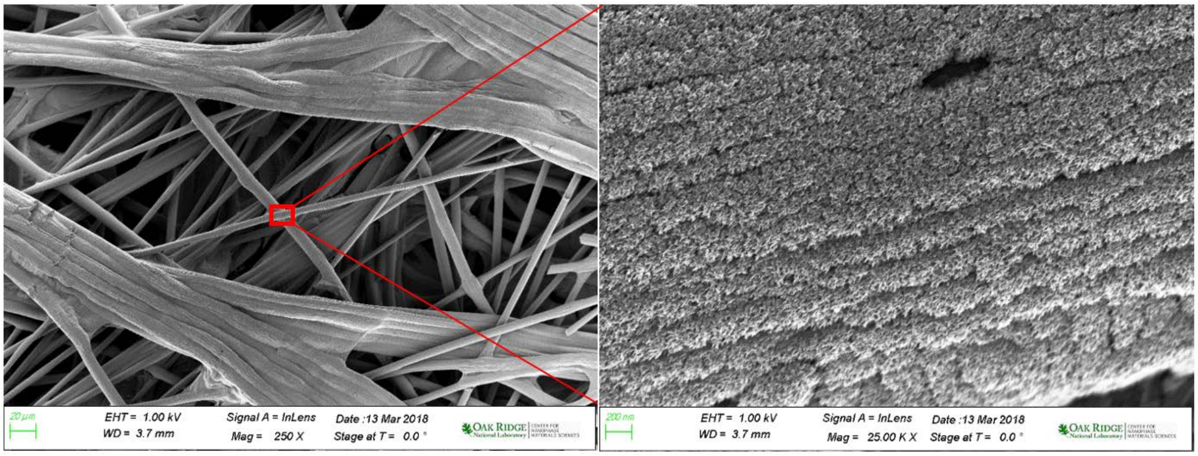

Figure 3. SEM images of CNS on carbon paper from graphite fibers (left, scale bar = 20 micrometers). High magnification image (right, scale bar = 200nm) shows intact CNS texture. The CNS appears to grow several microns into the carbon paper but does not permeate the entire paper.

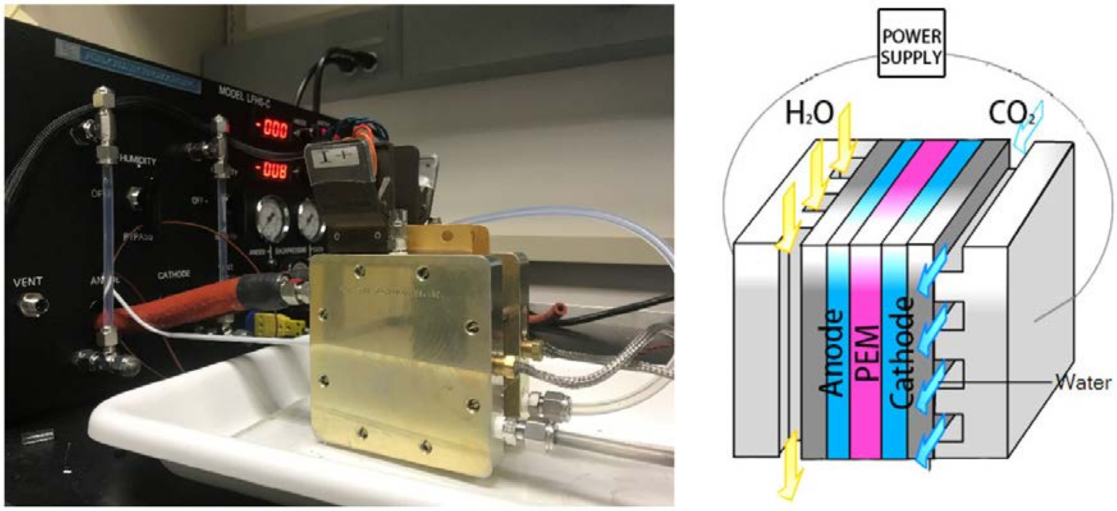

Figure 4. Image and schematic of the GDE cell for electrochemical CO_2RR. The system used here was an adapted H_2 fuel/electrolysis cell in which the cathode was outfitted with the CNS catalyst.

was composed of our catalyst on carbon paper as the cathode, a Pt/C/carbon cloth as the anode, and a Nafion 117 cation exchange membrane. CO_2RR and OER are the desired reactions for cathode and anode, respectively. The membrane allows protons to pass through while keeping the gases separate. Typically for this reaction we would use an anion exchange membrane (Selemion AMV), but because we had no experience running Selemion in a GDE, we decided to work with Nafion to minimize risk. Some effort was required to find the right type of carbon paper onto which we could grow the CNS layer, because many of the commonly used cloths and papers could not tolerate the plasma-enhance chemical vapor deposition required to grow CNS. Figure 3 shows SEM images of a successfully grown CNS layer on carbon cloth. CNS fully coats the fibers well into the paper, for at least several layers but does not fully penetrate the paper. Figure 4 depicts the cell used in this study and a schematic of a vapor phase cell construction.

Moisture is obligatory for both cathodic CO_2RR, as a proton source, and anodic OER from water oxidation, as well as to maintain ionic conductivity of the Nafion membrane. The humidity level was controlled with different temperatures and flow rates by a commercial humidification system designed by the fuel cell manufacturer.

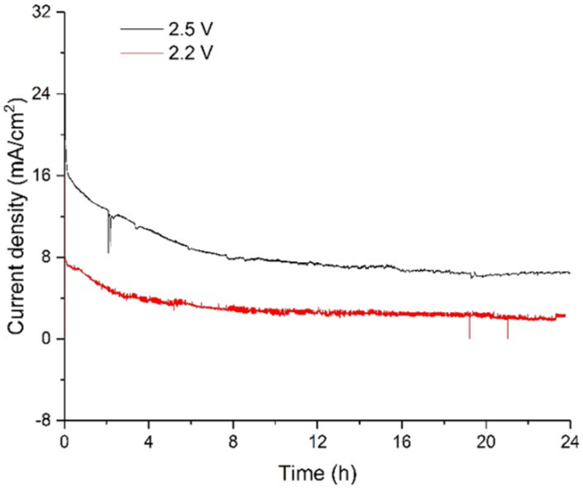

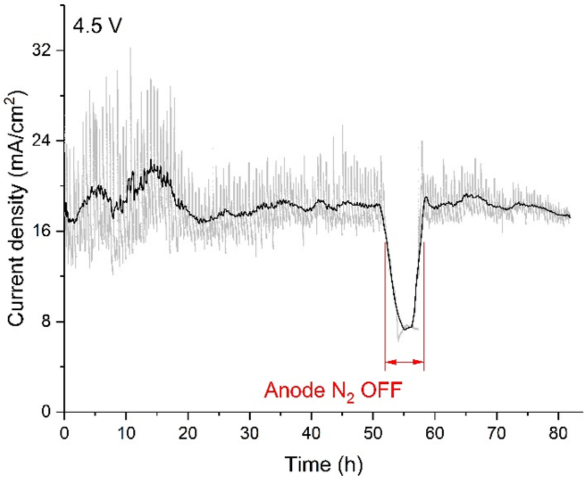

Figure 5. Current density at different full cell potentials for the GDE.

The overall current density in our previous study within $KHCO_3$ electrolyte was *ca.* 2 mA/cm^2 at 3.1 V full cell potential. In comparison, much higher current could be achieved with the vapor phase cell (Figure 5): 2.6 mA/cm^2 @ 2.2 V, and 8 mA/cm^2 @ 2.5 V. More importantly, The CNS is highly stable in this configuration. SEM images in Figure 6 show that the CNS remains intact after reaction at 4.5 V for 80 hours with a current density greater than 16 mA/cm^2. However, the graphite anode is not stable for OER, and a titanium anode was later required to be implemented; the anode compartment could also be modified to run with aqueous electrolyte as in a conventional electrochemical cell.

To collect any possible low vapor pressure hydrocarbon products, the post-reaction humidified CO_2 stream passed through two cold fingers at 0 ^oC (regular ice) and -77 ^oC (dry ice/ isopropanol), respectively. Gas chromatography was employed to separate and analyze gas phase products in-situ.

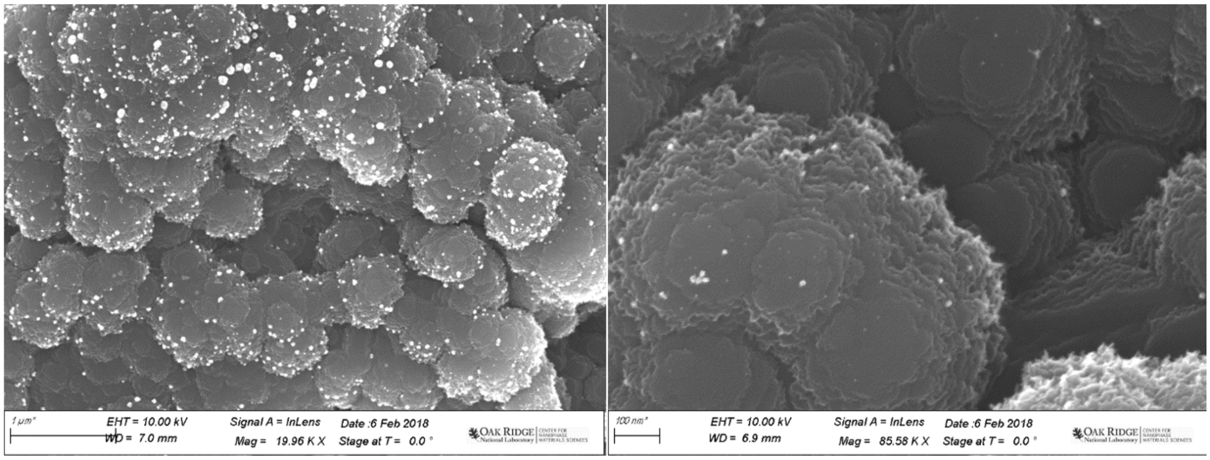

Figure 6. Representative SEM images of post reaction catalyst on carbon paper cathode running in the vapor phase. The bright dots are CuNPs. The texture of CNS remains intact (right panel) after reaction at 4.5 V for 80 h.

We observed that at 2.2 V, ethanol was detected as the only product in water that condensed at 0 ^oC from the post-reaction humidified CO_2 stream by NMR (Figure 7). At 2.5 V, ethanol was still the only product that collected in the cold trap at dry ice temperature. At 4.5 V, diverse hydrocarbon products were observed, and the major product was shifted to methanol, while

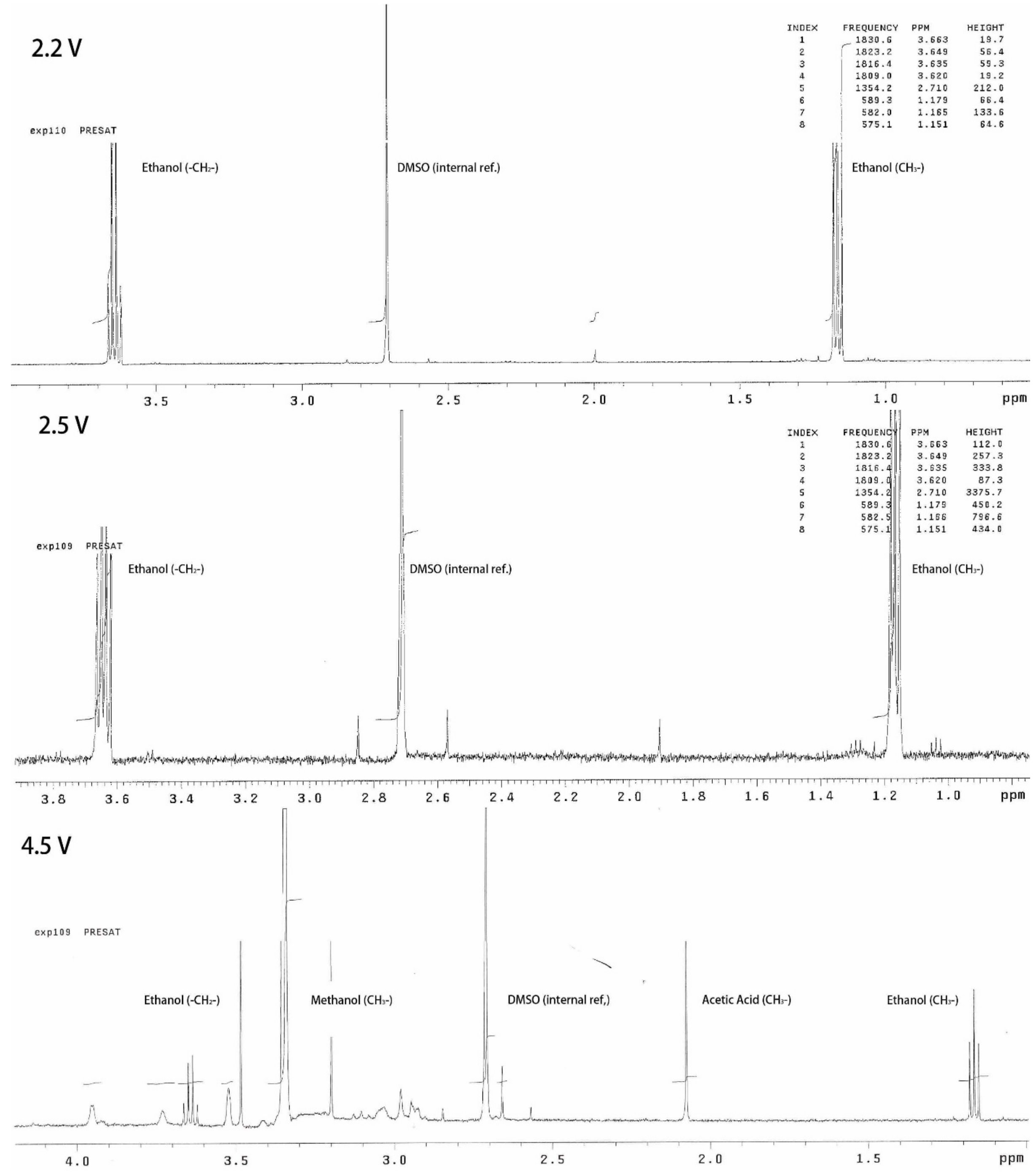

INDEX	FREQUENCY	PPM	HEIGHT
1	1830.6	3.663	19.7
2	1823.2	3.649	56.4
3	1816.4	3.635	59.3
4	1809.0	3.620	19.2
5	1354.2	2.710	212.0
6	589.3	1.179	66.4
7	582.0	1.165	133.6
8	575.1	1.151	64.6

INDEX	FREQUENCY	PPM	HEIGHT
1	1830.6	3.663	112.0
2	1823.2	3.649	257.3
3	1816.4	3.635	333.8
4	1809.0	3.620	87.3
5	1354.2	2.710	3375.7
6	589.3	1.179	450.2
7	582.5	1.166	796.6
8	575.1	1.151	434.0

Figure 7. NMR spectra of hydrocarbon products from vapor-phase operation of the catalyst at various potentials. At moderate voltages (2.2 V, 2.5 V) ethanol is the only condensable product.

ethanol, formic acid and acetic acid were also present. While these results are promising, the FE for hydrocarbon products is low (~ 3.1 %), and hydrogen was the major product with an estimated

FE of 95.6 % at 2.2 V. We believe that this is strictly a result of using proton-conducting Nafion rather than the anion-conducting Selemion that was used in the liquid phase work. However, we note that making a C2 product such as ethanol directly from CO_2 in the gas phase is a significant achievement, even at low Faradaic efficiency. However, there are several deficiencies with this study: first, due to the short-term nature of this project the reaction conditions are not optimized. Including cell temperature, humidity load on each compartment, flow rate and pressure through each compartment we have 7 physical variables that would need to be optimized. Further, the use of Nafion membrane, which allows too many protons to access the cathode, resulted in significant excess hydrogen production. We likewise did not test coatings on the GDE such as Teflon or hydroxide which can improve moisture management. These deficiencies are opportunities for future improvements.

Trace Contaminants

We studied on the impact of SO_x and NO_x contaminants that would be expected to be present in flue gas. We have tested a mixed gas [CO_2 (80%), CO (10%), NO (2%), SO_2 (1%), and balanced with N_2 (7%)] to mimic raw flue gas released from coal combustion. In a typical experiment, the 0.1 M $KHCO_3$ electrolyte was first saturated by pure CO_2, and then purged by the mixed gas. The pH of electrolyte dropped from 6.8 to 2.3 due to the hydrolysis of NO and SO_2, resulting in acid. Using a planar electrode identical to that published in the original study, massive gas bubbles were observed from electrode surface at -1.9 V vs. Ag/AgCl due to low pH that promotes competitive hydrogen evolution. No ethanol or other hydrocarbon products were detected from the post-reaction electrolyte after a 6-hour experiment, indicating that CO_2RR was inhibited; However,

NH_4^+ was presented in the NMR spectrum as a product NO reduction. Examining each contaminant individually, we conducted proxy experiments with nitrate and sulfate (as pH neutral proxies for NO_x and SO_x) to better understand inhibition. Multiple runs with 10 mM nitrate (NO_3^-) confirmed that the presence of nitrate can inhibit the reaction consistent with the observation regarding NO, as no ethanol was detected from the electrolyte even after 18 hours. Interestingly, no ammonia/ammonium but only trace nitrite (NO^{2-}) was observed. Although the mechanism is unknown, the pH might be critical in denitrification since a significant difference in pH was observed between the two experiments. Regarding ammonia or ammonium inhibition of the reaction, Lalitha et al (*3*) suggest that charged nitrogen species such as ammonium are capable of passivating the surface of copper against electrochemical reactions. As copper is required in our catalyst to facilitate dimerization of carbon monoxide, copper inhibition would eliminate ethanol as a product.

For SO_x contaminants, we also employed 10 mM sulfate (SO_4^{2-}) as a proxy, which was added to the $KHCO_3$ electrolyte and run with the catalyst. Under optimal conditions with no contaminants, we expect Faradaic efficiencies in the range of 60-65%. After 6 hours with sulfate contamination, ethanol was produced but at a reduced FE of approximately 55%

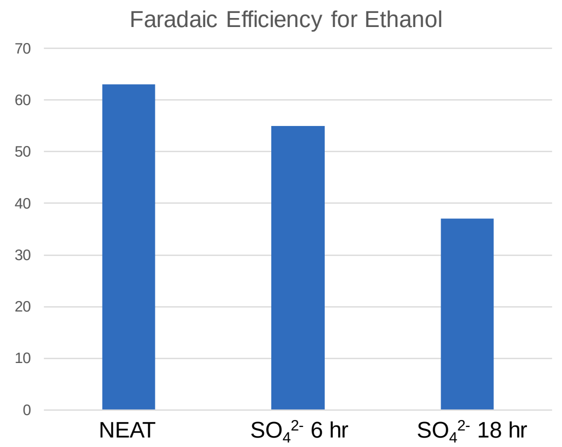

Figure 8. Sulfate 10 mM in the electrolyte slowly poisons the catalyst resulting in reduced product formation.

(Figure 8). After 18 hours, the FE is further reduced to 37.5 %. Trace acetic acid is present which suggests that reduction is slowing (Figure 9).

In order to better understand the role of sulfate we conducted x-ray photoelectron analysis (XPS) on the contaminated electrode. The finding that sulfate can inhibit the reaction was surprising, as the copper nanoparticles are deposited in situ from a copper sulfate/sulfuric acid solution and sulfate ion is expected to be present in trace amounts at all times.

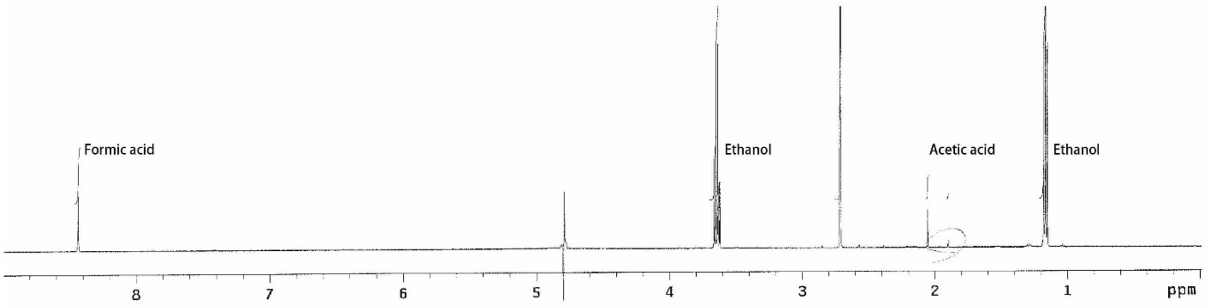

Figure 9. Example NMR spectrum of hydrocarbon products in post-reaction electrolyte with 10 mM SO_4^{2-}.

XPS analysis of a contaminated electrode (Figure 10) indicates the presence of copper sulfide, or some types of sulfide species on the electrode surface. XPS further suggests that the copper is largely in the metallic, unoxidized form. Electrochemical reduction of SO_4^{2-} to S^{2-} is unusual, but could be a result of the intense electric fields produced by each individual nanospike (*4*). We interpret these results to be that a CuS crust is forming on the surface of the Cu nanoparticles, passivating the surface against CO adsorption and limiting electron transfer. An examination of the eH-pH diagram (*5*) suggests that at our Cu deposition potential (-0.8 V vs Ag/AgCl) and pH, sulfide formation is less likely but possible, but that at our operational potential (-1.9 V vs Ag/AgCl) sulfide formation is more likely. All together these findings suggest that SO_x is tolerated for some time but is not ideal.

In a real-world application both SO_x and NO_x would be minimized due to scrubbing and the amine CO_2 adsorbent, but would not likely be absolute zero. Fouling of the catalyst appears to be limited to the copper nanoparticle, so periodic refreshing of the copper nanoparticle in situ through electrochemical oxidation and reprecipitation would be a strategy to eliminate accumulated poisons. The CNS layer does not appear to be sensitive to either contaminant.

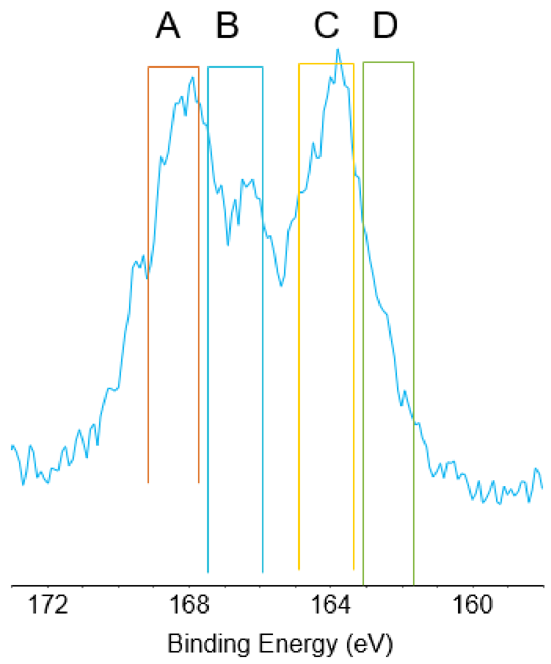

Figure 10. XPS describes oxidation and binding states for individual elements. Identified species in a sulfur-contaminated electrode include (A) B.E. = 168.0 eV - sulfate, SO_4^-, (B) B.E. = 165.8 eV to 166.4 eV - SO_3^- or SO_2^-, (C) B.E. = 163.4 to 163.6 eV - metal sulfide, likely Cu-sulfide, (D) B.E. = 162.0 eV - metal sulfide, likely Cu-sulfide.

Summary

In the course of this project we have studied strategies to improve current density through improved electrolyte to electrode contact and have examined the effects of two important potential classes of contaminants likely to be present in trace amounts in fossil flue gas. Our results indicate that a likely pathway towards higher current density operation is to implement the catalyst in a gas phase reactor. We have demonstrated that operation of the catalyst in the gas phase is possible but we have not yet optimized the conditions due to a large number of variables.

Trace contaminant studies suggest that nitrogen species are likely to be very limiting and sulfur species are somewhat limiting. Either of these contaminants are also problematic for amine-based sorbents, and utilities that would implement an electrochemical catalyst are likely going to take steps to reduce their presence. However, even at ppm levels we would expect based on these results to see a cumulative effect, which could be mitigated by periodic refreshing of the copper co-catalyst nanoparticles in situ via electrochemical means.

1. Y. Song *et al.*, High-Selectivity Electrochemical Conversion of CO2 to Ethanol using a Copper Nanoparticle/N-Doped Graphene Electrode. *ChemistrySelect* **1**, 6055-6061 (2016).
2. L. B. Sheridan *et al.*, Growth and Electrochemical Characterization of Carbon Nanospike Thin Film Electrodes. *J. Electrochem. Soc.* **161**, H558-H563 (2014).
3. A. Lalitha, S. Ramesh, S. Rajeswari, Surface protection of copper in acid medium by azoles and surfactants. *Electrochim. Acta* **51**, 47-55 (2005).
4. Y. Song *et al.*, A physical catalyst for the electrolysis of nitrogen to ammonia. *Science Advances* **4**, (2018).
5. R. Woods, R. Yoon, C. Young, Eh-pH diagrams for stable and metastable phases in the copper-sulfur-water system. *International journal of mineral processing* **20**, 109-120 (1987).